Paper No.
2348

NACE INTERNATIONAL CORROSION 2013 CONFERENCE & EXPO

Effect of pH on CO_2 Corrosion of Mild Steel at Elevated Temperatures

Tanaporn Tanupabrungsun, Bruce Brown, Srdjan Nesic

Institute for Corrosion and Multiphase Technology
Department of Chemical & Biomolecular Engineering
Ohio University, Athens, OH 45701, USA

ABSTRACT

Electrochemical and surface analysis techniques were used to study the mechanisms of CO_2 corrosion of mild steel over the temperature range of 80-200°C. Experiments were carried out in a 4-liter autoclave equipped to perform *in situ* electrochemical measurements using linear polarization resistance (LPR) and electrochemical impedance spectroscopy (EIS). The electrolyte was 1 wt.% NaCl saturated with CO_2 at 0.030 M of $[CO_2]_{aq}$. Corrosion tests were conducted at temperatures of 80, 120, 150 and 200°C; pH values of 4.0 and 6.0 were used. After the experiments, sample surfaces were characterized via scanning electron microscopy (SEM) and X-ray diffraction (XRD). The results showed that the corrosion rates decreased with time due to formation of corrosion products. Corrosion rates at pH 4.0 are higher than those at pH 6.0 for each temperature. For the test series at both pH 4.0 and pH 6.0, the final corrosion rates decreased with temperature because increasingly protective layers formed on the steel surface. Analysis of the corrosion products confirmed that $FeCO_3$ layers were observed for all the tests and that there was a mixture of Fe_3O_4 and $FeCO_3$ at temperatures above 150°C.

Key words: CO_2 corrosion, elevated temperature, mild steel, electrochemical measurements

INTRODUCTION

CO_2 corrosion of mild steel in the oil and gas industry has been widely investigated. Nevertheless, research in high temperature CO_2 corrosion (>100°C) has been rarely conducted, due to the complexity involved, and the corrosion mechanism and influential factors remain unclear. At temperatures below 100°C the mechanisms of CO_2 corrosion in aqueous environments are known with more certainity.[1-5] The main anodic and cathodic reactions are listed in Table 1. For CO_2 corrosion of mild steel, the main anodic reaction is iron oxidation and the main cathodic reactions are the hydrogen evolution from H^+, H_2CO_3 and H_2O.

Table 1
Electrochemical Reactions for CO_2 Corrosion

	Name	Reaction
Cathodic reactions	H^+ reduction	$2H^+_{(aq)} + 2e^- \rightarrow H_{2(g)}$
	H_2CO_3 reduction	$2H_2CO_{3(aq)} + 2e^- \rightarrow 2HCO^-_{3(aq)} + H_{2(g)}$
	H_2O reduction	$2H_2O_{(l)} + 2e^- \rightarrow 2OH^-_{(aq)} + H_{2(g)}$
Anodic reaction	Fe oxidation	$Fe \rightarrow Fe^{2+}_{(aq)} + 2e^-$

When mild steel corrodes, it releases Fe^{2+} ions which accumulate in the solution. When their concentration reaches and exceeds the saturation level, $FeCO_{3(s)}$ will precipitate according to:

$$Fe^{2+}_{(aq)} + CO^{2-}_3 \rightarrow Fe\,CO_{3(s)}$$

and cover the steel surface what may lower the corrosion rate. The driving force for precipitation is the supersaturation level, defined as:

$$S = \frac{C_{Fe^{2+}} C_{CO_3^{2-}}}{K_{SP}} \quad (1)$$

where c corresponds to concentration and K_{sp} is the solubility limit of $FeCO_3$.

The effect of pH on CO_2 corrosion at temperatures up to 100°C has been described by Nesic, *et al.*[6] pH has a significant direct effect on the corrosion rate and indirect influence on $FeCO_3$ formation: the higher the pH, the less corrosive the system is as there are fewer H^+ ions in solution and the solubility of $FeCO_3$ decreases, leading to supersaturation and a high precipitation rate. The mechanisms of corrosion and the effect of key parameters are less understood above 100°C. To get a better insight into the effect of pH on CO_2 corrosion of mild steel over a range of above 100°C, electrochemical measurements have been used here.

METHODOLOGY

Experiments were carried out in a 4-liter autoclave equipped to perform *in situ* electrochemical measurements. The electrolyte was 1 wt.% NaCl saturated with CO_2. To study the effect of temperature on CO_2 corrosion, the dissolved CO_2 concentration needs to be controlled to eliminate the temperature effect on the CO_2 solubility. In addition, the dissolved CO_2 represents the total amount of weak acid in the system, so it is the best controlling parameter. Thus, the concentration of dissolved CO_2 was fixed at 0.030M for each experiment. For this condition, the partial pressure of CO_2 is as listed in Table 2. An autoclave system is used to control the system at different temperatures. The speciation was calculated using the equilibrium constants for a CO_2-H_2O system in the open literature.[7] Corrosion tests were conducted at temperatures of 80, 120, 150 and 200°C, pH values of 4.0 and 6.0 were used. A high temperature/pressure ZrO_2-based pH probe was used for monitoring pH. Two types of API* 5L X65 (UNS K03014) samples were employed: 1) cylindrical specimens (1.0 cm. in diameter and 2.0 cm in height) for the electrochemical measurement and weight loss and 2) flat square specimens (1.25 cm x 1.25 cm x 0.2 cm) for surface analysis. A Gamry† Reference 600™ potentiostat, with DC105 and EIS300 V5.30 software packages, was used for linear polarization resistance (LPR) and electrochemical impedance spectroscopy (EIS) measurements. Corrosion rates from LPR were

* American Petroleum Institute, 1220 L Street, NW Washington, DC 20005-4070
† Trade name

calculated using B = 26 mV/decade.[8] After 20 hour tests, the specimens were analyzed by scanning electron microscopy (SEM), energy-dispersive X-ray spectroscopy (EDX) and X-ray diffraction (XRD).

Table 2
Effect of Temperature on CO_2 Solubility and Pressure

T (°C)	$CO_{2\,(aq)}$ (molar)	pCO_2 (bar)	Total pressure (bar)
25	0.030	0.97	1.0
80	0.030	2.2	2.7
120	0.030	3.2	5.2
150	0.030	3.7	8.4
200	0.030	3.8	19.3

RESULTS AND DISCUSSION

Electrochemical Experiments and Surface Characterization

The effects of pH on CO_2 corrosion at temperatures of 80, 120, 150 and 200°C are summarized in Figure 1 a) and b). Starting with 80°C, at pH 4.0, the corrosion rate remained constant with time. The EIS results are shown in Figure 2a). The Nyquist plot represents corrosion behavior indicative of the charge transfer process. The SEM image in Figure 3a) shows a uniformly corroded steel surface, and only iron was detected by EDX. In contrast, the corrosion rate at pH 6.0 in Figure 1b) was initially high and then decreased with time, due to the formation of a protective $FeCO_3$ layer. The Nyquist plots in Figure 2b) at 0 – 8 hours show semi-circles, which is the characteristic of Faradaic impedance implying charge transfer controlled corrosion phenomena.[9, 10] However, at 20 hours it changed to a double semi-circle, which indicated mass transfer dependence. In other words, the steel surface was covered by a corrosion product layer as seen in the SEM image (Figure 3b).

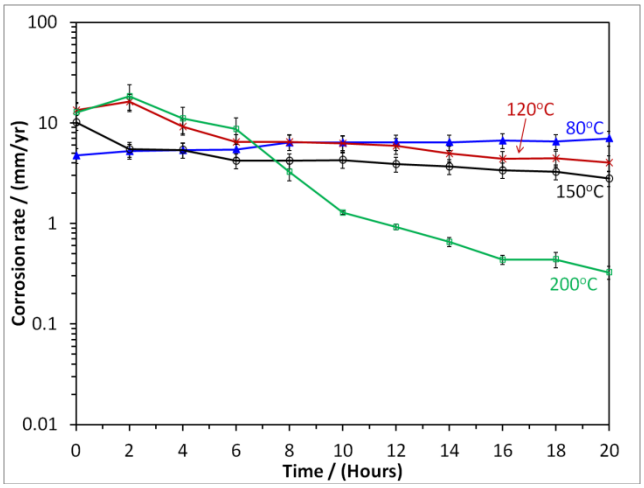

a) pH 4.0

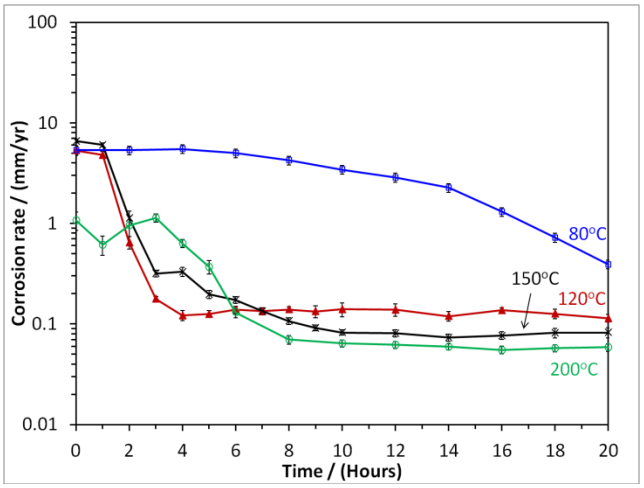

b) pH 6.0

Figure 1: LPR Corrosion Rate over Time; T=80-200°C, $[CO_2]_{aq}$ =0.030M.

At 120°C, the measured corrosion rates at pH 4.0 and 6.0 were the highest at the beginning, and then decreased with time as illustrated in Figure 1a) and b). For EIS analysis (Figure 4a and b), the Nyquist plots indicated diffusion control for both cases at low frequency. However, the resistance in the test at pH 6.0 was two orders of magnitude higher than that at pH 4.0. This is due to the formation of $FeCO_3$ scales, as presented in Figure 5a) and b). The $FeCO_3$ scales at pH 6.0 more thoroughly covered the steel surface than those at pH 4.0. Therefore, the corrosion rate at pH 6.0 was lower than that at pH 4.0.

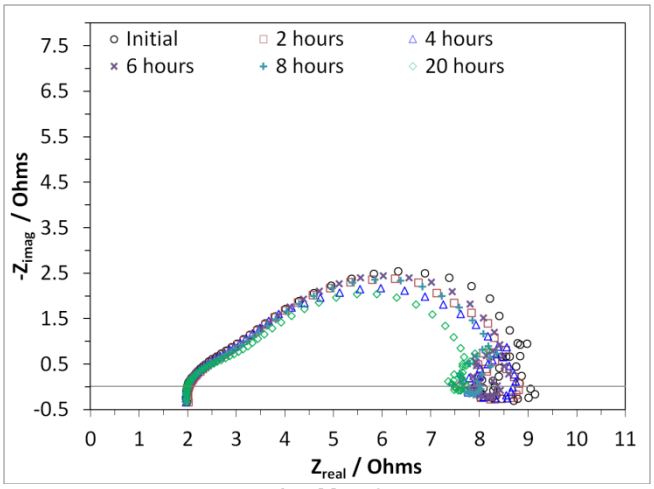

a) pH 4.0

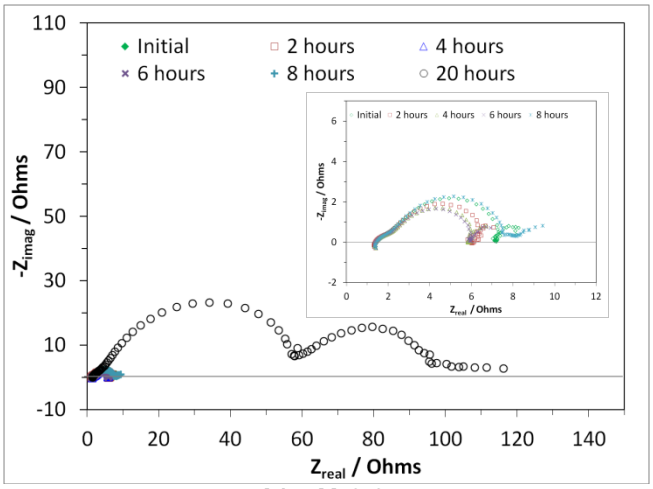

b) pH 6.0

Figure 2: EIS at 80°C, 20 Hours

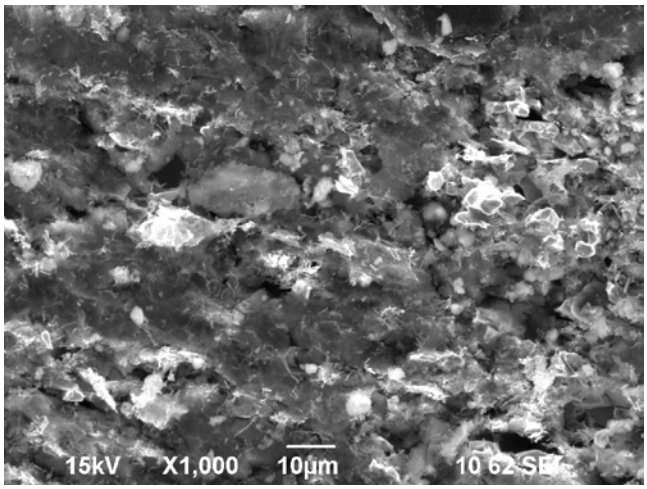

a) pH 4.0

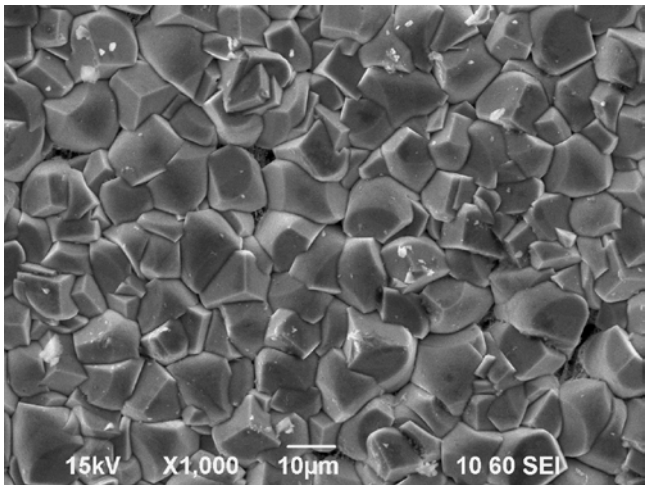

b) pH 6.0

Figure 3: SEM Images at 80°C, 20 Hours

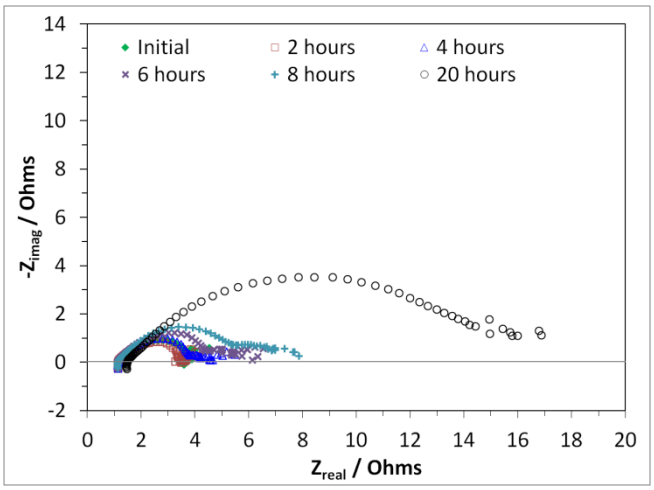

a) pH 4.0

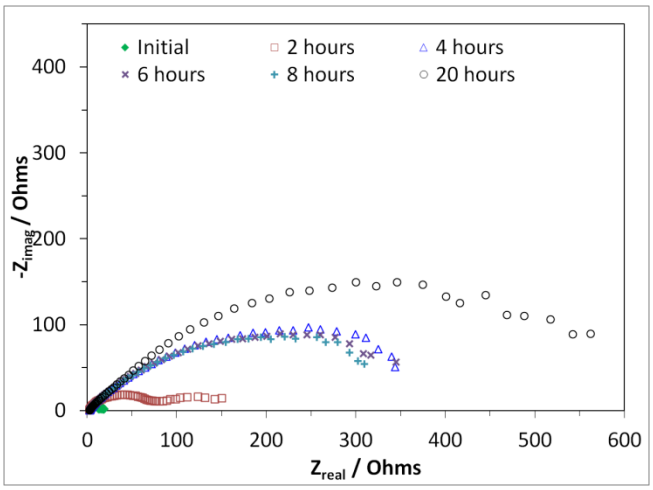

b) pH 6.0

Figure 4: EIS at 120°C, 20 Hours

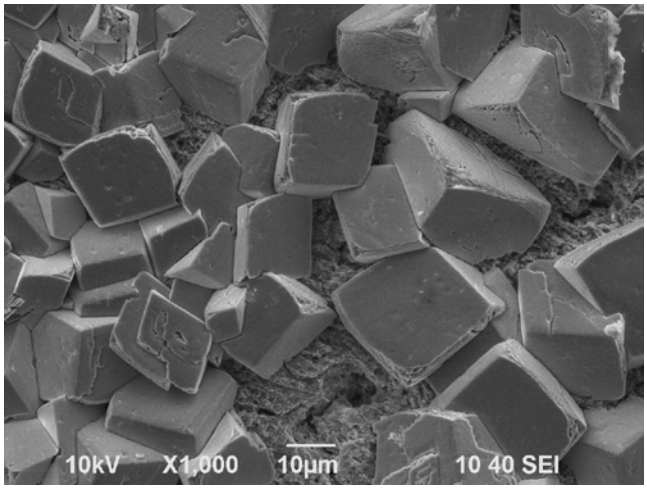

a) pH 4.0

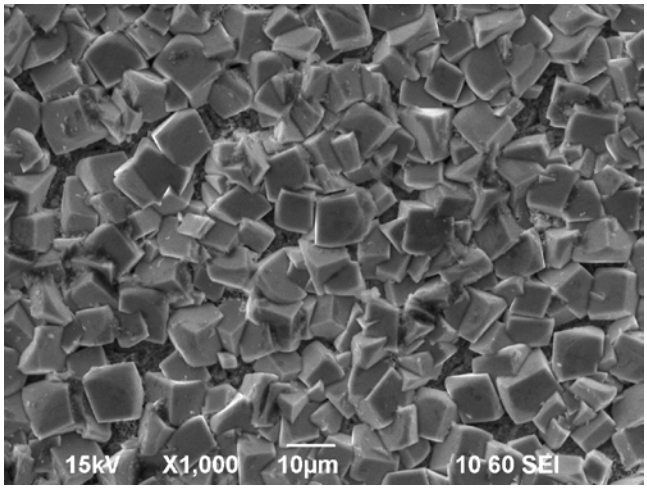

b) pH 6.0

Figure 5: SEM Images at 120°C, 20 Hours

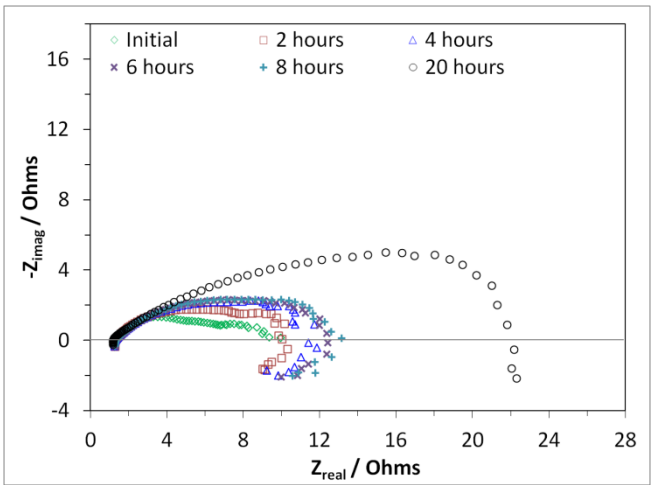

a) pH 4.0

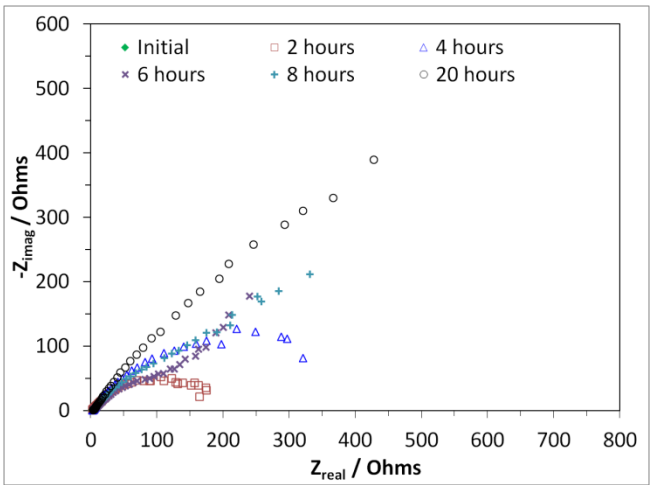

b) pH 6.0

Figure 6: EIS at 150°C, 20 Hours

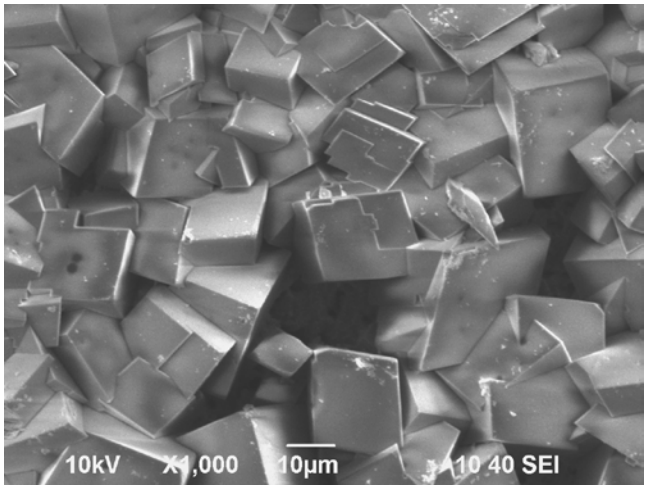

a) pH 4.0

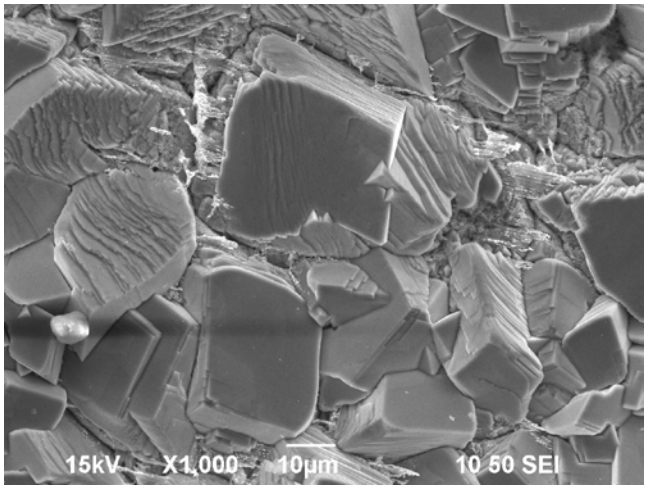

b) pH 6.0

Figure 7: SEM Images at 150°C, 20 Hours

At 150°C and 200°C, similar results were obtained for both pH 4.0 and 6.0 to those results at 120°C: the corrosion rates (Figure 1a and b), the Nyquist plots (Figure 6 and Figure 8), the surface morphology

(Figure 7 and Figure 9). The corrosion rates at pH 4.0 were higher than those at pH 6.0. The diffusion control appears on the Nyquist plots for both cases. The steel surfaces were covered by corrosion products. However, at pH 4.0 the Nyquist plots show an inductance behavior at low frequency at both 150°C and 200°C, which represents a multi-step process or any reaction that has intermediate steps, such as iron dissolution and magnetite formation.[11-14] At pH 6.0, the inductance loops did not appear on the Nyquist plot. This may be due to much larger value for the resistance (real part) than on the reactance (imaginary part). The corrosion product layers developed at 200°C offered protection that was superior to that observed at lower temperatures.

For surface analysis, the steel surfaces for the experiments at 120, 150 and 200°C at the pH value of 4.0 were analyzed by XRD, as shown in Figure 10a), b) and c), respectively. The results show that $FeCO_3$ was the main corrosion product at 120°C. A mixture of $FeCO_3$ and Fe_3O_4 was found at 150°C and 200°C.

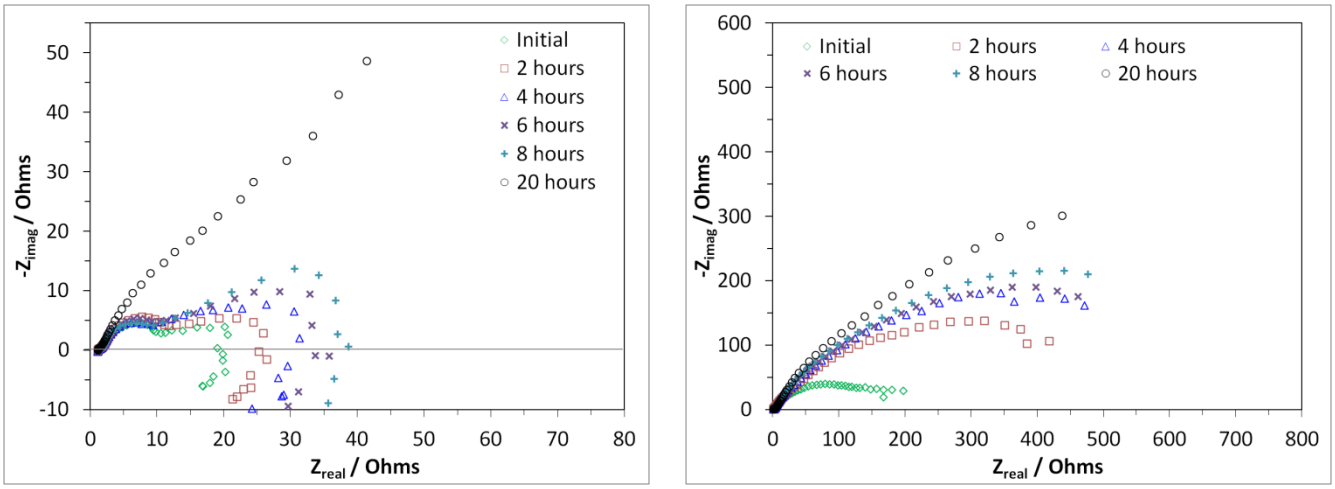

a) pH 4.0 b) pH 6.0

Figure 8: EIS at 200°C, 20 Hours

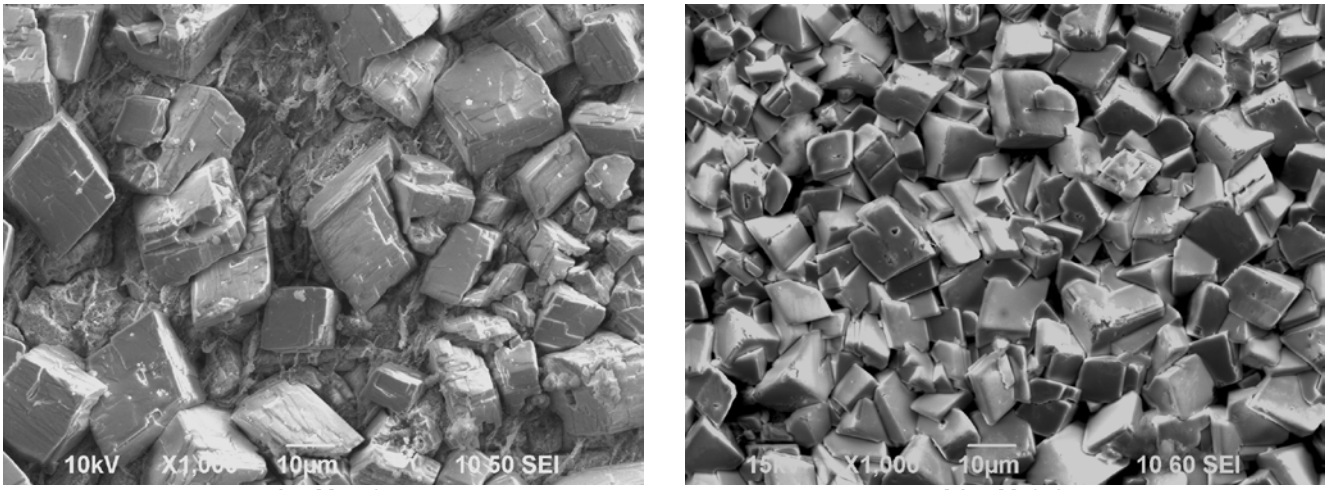

a) pH 4.0 b) pH 6.0

Figure 9: SEM Images at 200°C, 20 Hours

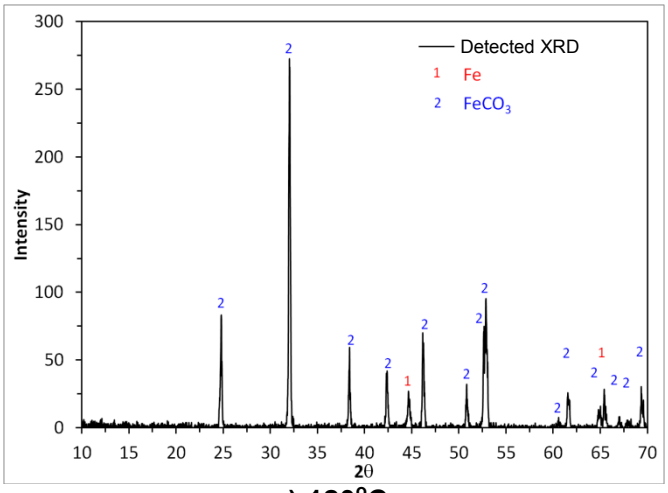

a) 120°C

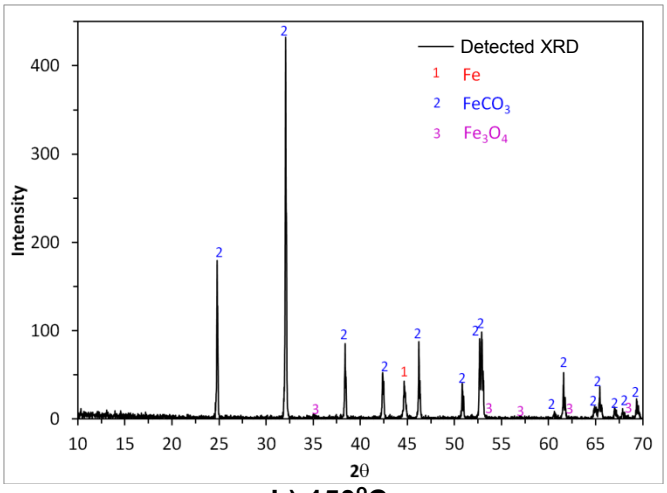

b) 150°C

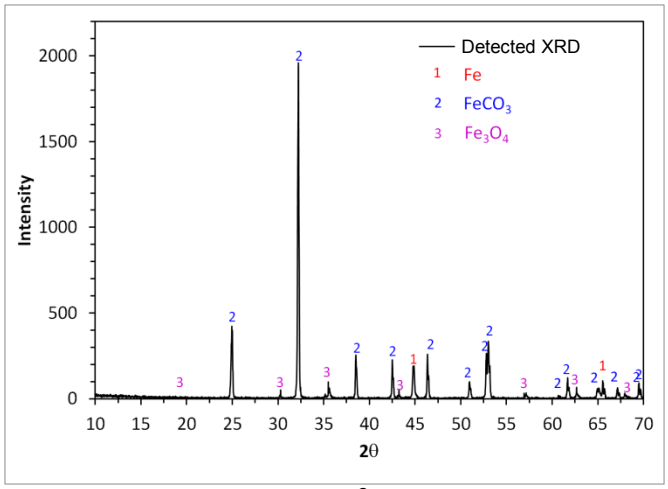

c) 200°C

Figure 10: XRD Analysis at pH 4.0 after 20 Hours

In all cases, the initial corrosion rates were much higher, releasing more corrosion products into the aqueous solution making the formation of $FeCO_3$ kinetically favorable.[15, 16] The higher the temperature, the higher the initial corrosion rate, as expected. However, the kinetics of $FeCO_3$ precipitation also increases with temperature.[17] Consequently, the corrosion rate is lowered because $FeCO_3$ forms on the steel surface and acts as a diffusion barrier.[18, 19] At 80°C and pH 4.0, the condition was thermodynamically unfavorable for $FeCO_3$ formation, so there was no $FeCO_3$ found on the steel surface. However, the equilibrium of $FeCO_3$ formation is shifted to lower pH when temperature increases.[20, 21] In other words, at higher temperature it is easier to reach saturation with respect to $FeCO_3$ even at lower pH. At temperatures above 150°C, Fe_3O_4 is thermodynamically favored.[20, 21] Therefore, a mixture of $FeCO_3$ and Fe_3O_4 was observed.

Proposed Mechanisms for CO_2 Corrosion at 25-200°C

Based on the experimental results above, four types of processes need to be considered as important for the CO_2 corrosion mechanism of mild steel at high temperature, as shown in Figure 11:

1. Chemical equilibria in a CO_2 system[7]

In a CO_2-H_2O-NaCl system, four homogeneous chemical reactions need to be considered.

- gaseous CO_2 dissolves in solution,

- dissolved CO_2 is hydrated to form aqueous H_2CO_3,
- aqueous H_2CO_3 dissociates to HCO_3^- and H^+,
- aqueous HCO_3^- dissociates to CO_3^{2-} and H^+.

All of these reactions are comparatively fast and can be considered to be in equilibrium. Since they are linked *via* common species, such as H^+, changing any one concentration will shift the equilibrium concentration for all the others.

2. Corrosion processes

When mild steel is in a corrosive environment, such as an acidic aqueous CO_2 systems, corrosion will occur. For CO_2 corrosion of mild steel, the anodic reaction is iron oxidation and the cathodic reactions are the hydrogen evolution from H^+, H_2CO_3 and H_2O, as listed in Table 1. The kinetic rates of these reactions increase with temperature resulting in higher corrosion rate.

3. $FeCO_3$ formation

When steel corrodes, it releases Fe^{2+}. Once conditions for forming $FeCO_3$ are achieved (concentration of species is above saturation level), $FeCO_3$ will form and cover the steel surface, thereby lowering the corrosion rate. The solubility constant K_{sp} depends on temperature. For example, at 25-80°C, $FeCO_3$ precipitates only at elevated pH and/or high concentration of Fe^{2+}. As temperature is increased, $FeCO_3$ also precipitates at lower pH. For example, $FeCO_3$ was observed only at pH 6.0 at 80°C, whereas it was present at also at pH 4.0 at 120°C. Temperature accelerated the precipitation kinetics of $FeCO_3$, making it more protective.

4. Fe_3O_4 formation

At high temperatures (>100°C) and typical operating conditions, there are two types of corrosion products which can appear, $FeCO_3$ and Fe_3O_4. Which one will dominate depends on the thermodynamics and kinetics of their formation. For instance, at low pCO_2 (<1 bar) and 200°C, only Fe_3O_4 forms on the steel surface.[20] Due to the very fast kinetics. However, at higher partial pressures of CO_2, (e.g. at pCO_2 > 3 bars at 150°C), $FeCO_3$ and Fe_3O_4 may coexist on the steel surface.

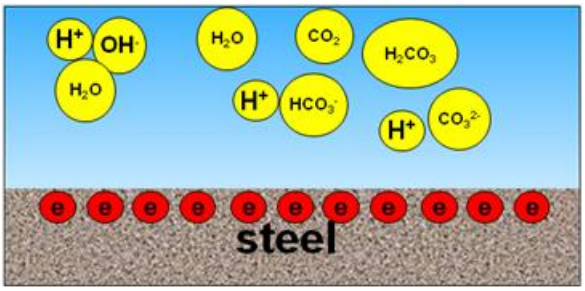

1: Equilibria for an aqueous CO_2 system

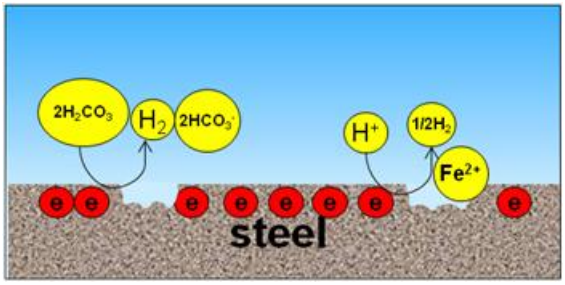

2: Electrochemical corrosion process

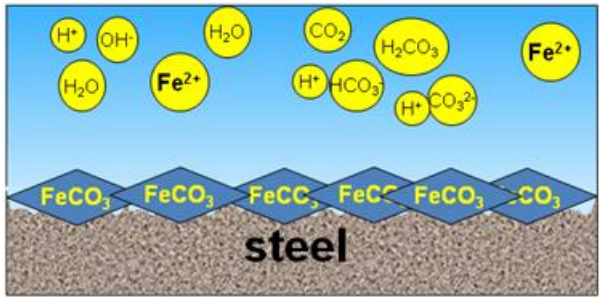

3: $FeCO_3$ formation

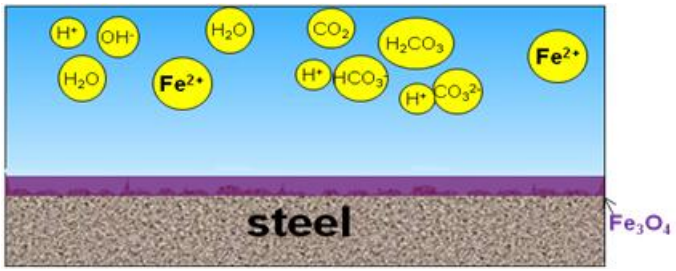

4a: Fe_3O_4 formation

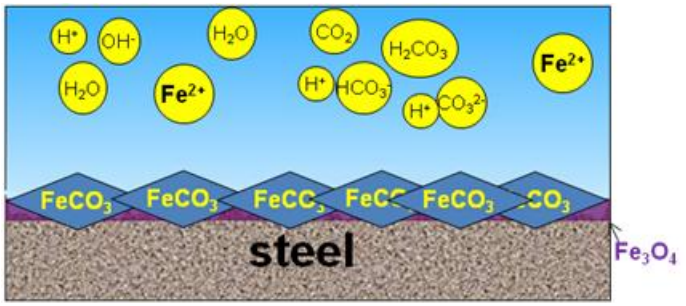

4b: Combined $FeCO_3$ and Fe_3O_4 formation at elevated pCO_2

Figure 11: Schematic of various processes comprising the mechanism of CO_2 corrosion at high temperatures (up to 200°C).

CONCLUSIONS

- Corrosion rates at pH 4.0 are higher than those at pH 6 over the whole temperature range tested here: 80-200°C.
- At temperatures above 120°C, corrosion rate more readily decreases with time due to formation of corrosion products.
- $FeCO_3$ was the main corrosion product for all test conditions. It was not found only at pH 4.0 and 80°C where the solution was not saturated with respect to $FeCO_3$,
- At temperatures above 150°C, a small amount of Fe_3O_4 was detected along with $FeCO_3$, both at pH 4.0 and pH 6.0.

ACKNOWLEDGEMENTS

The authors would like to thank the following companies for their financial support: BG Group, BP, Champion Technologies, Chevron, Clariant Oil Services, ConocoPhillips, Encana, ENI S.P.A., ExxonMobil, WGIM, NALCO Energy Services, Occidental Oil Company, Petrobras, PETRONAS, PTT, Saudi Aramco, INPEX Corporation, Total, TransCanada. The authors also thank Brian Hassler of the

Center for Electrochemical Engineering Research (CEER), Department of Chemical and Biomolecular Engineering, Ohio University, for his help with the XRD measurements.

REFERENCES

1. C. de Waard and D. E. Milliams, “Carbonic acid corrosion of steel,” Corrosion, vol. 31, no. 5, pp. 177–181, 1975.

2. L. G. S. Gray, B. G. Anderson, M. J. Danysh, and P. R. Tremaine, “Mechanism of carbon steel corrosion in brine containing dissolved carbon dioxide at pH 4,” in Corrosion 89, 1989, Paper no. 464.

3. L. G. S. Gray, B. G. Anderson, M. J. Danysh, and P. R. Tremaine, “Effect of pH and temperature on the mechanism of carbon steel corrosion by aqueous carbon dioxide,” CORROSION/90, Paper no. 40, 1990.

4. S. Nesic, M. Nordsveen, and A. Stangeland, “A mechanistic model for CO_2 corrosion with protective iron carbonate scale films,” NACE Paper No. 01040. 2001.

5. S. Nesic, J. Postlethwaite, and S. Olsen, “An electrochemical model for prediction of corrosion of mild steel in aqueous carbon dioxide solutions,” Corrosion, vol. 52, no. 4, pp. 280–294, 1996.

6. S. Nesic, “Key issues related to modeling of internal corrosion of oil and gas pipelines – A review,” Corrosion Science, vol. 49, no. 12, pp. 4308–4338, 2007.

7. S. Nesic, M. Nordsveen, R. Nyborg, and A. Stangeland, “A mechanistic model for carbon dioxide corrosion of mild steel in the presence of protective iron carbonate films - Part 1: Theory and verification,” Corrosion, vol. 59, no. 5, pp. 443–456, 2003.

8. H. Fang, “Low temperature and high salt concentration effects on general CO_2 corrosion for carbon steel,” Ohio University, 2006.

9. I. Epelboin and M. Keddam, “Faradaic impedances: diffusion impedance and reaction impedance,” Journal of the Electrochemical Society, vol. 117, p. 1052, 1970.

10. I. Epelboin, M. Keddam, and H. Takenouti, “Use of impedance measurements for the determination of the instant rate of metal corrosion,” Journal of Applied Electrochemistry, vol. 2, no. 1, pp. 71–79, 1972.

11. M. Keddam, O. R. Mattos, and H. Takenouti, “Reaction model for iron dissolution studied by electrode impedance I . Experimental results and reaction model,” Journal of The Electrochemical Society, vol. 6, no. 2, pp. 257–266, 1981.

12. G. Baril, G. Galicia, C. Deslouis, N. Pébère, B. Tribollet, and V. Vivier, “An impedance investigation of the mechanism of pure magnesium corrosion in sodium sulfate solutions,” Journal of The Electrochemical Society, vol. 154, no. 2, pp. C108–C113, 2007.

13. F. Sweeton and C. Baes, “The solubility of magnetite and hydrolysis of ferrous ion in aqueous solutions at elevated temperatures,” The Journal of Chemical Thermodynamics, vol. 2, no. 4, pp. 479–500, 1970.

14. S. E. Ziemniak, M. E. Jones, and K. E. S. Combs, “Magnetite solubility and phase stability in alkaline media at elevated temperatures,” Journal of Solution Chemistry, vol. 24, no. 9, pp. 837–877, 1995.

15. C. de Waard, U. Lotz, and D. E. Milliams, “Predictive model for CO_2 corrosion engineering in wet natural gas pipelines,” Corrosion, vol. 47, no. 12, pp. 976–985.

16. A. Dugstad, “Mechanism of protective film formation during CO_2 corrosion of carbon steel,” CORROSION/98, Paper No. 31, 1998.

17. W. Sun and S. Nesić, “Kinetics of corrosion layer formation: Part 1—Iron carbonate layers in carbon dioxide corrosion,” Corrosion, vol. 64, no. 4, p. 334, 2008.

18. S. Nesic and K. L. J. Lee, “A mechanistic model for carbon dioxide corrosion of mild steel in the presence of protective iron carbonate films - Part 3: Film growth model,” Corrosion, vol. 59, no. 7, pp. 616–628, 2003.

19. W. Sun, S. Nesic, and R. C. Woollam, “The effect of temperature and ionic strength on iron carbonate ($FeCO_3$) solubility limit,” Corrosion Science, vol. 51, no. 6, pp. 1273–1276, 2009.

20. T. Tanupabrungsun, D. Young, B. Brown, and S. Nesic, “Construction and verification of pourbaix diagrams for CO_2 corrosion of mild steel valid up to 250°C,” CORROSION/2012, 2012.

21. M. Ueda, “Potential-pH diagram at elevated temperatures for metal-CO_2/H_2S-water systems and the application for corrosion of pure iron,” Corrosion Engineering, vol. 44, pp. 159–174, 1995.